

Some Novel Gas-Based Detection Techniques

Graham C. Smith

Brookhaven National Laboratory, Upton NY 11973

- Gas Electron Multipliers (GEMs)
- Pin Detectors
- Micromegas (μ CAT)
- Even MWPCs!
- Operation in Ionization Mode (n & γ)

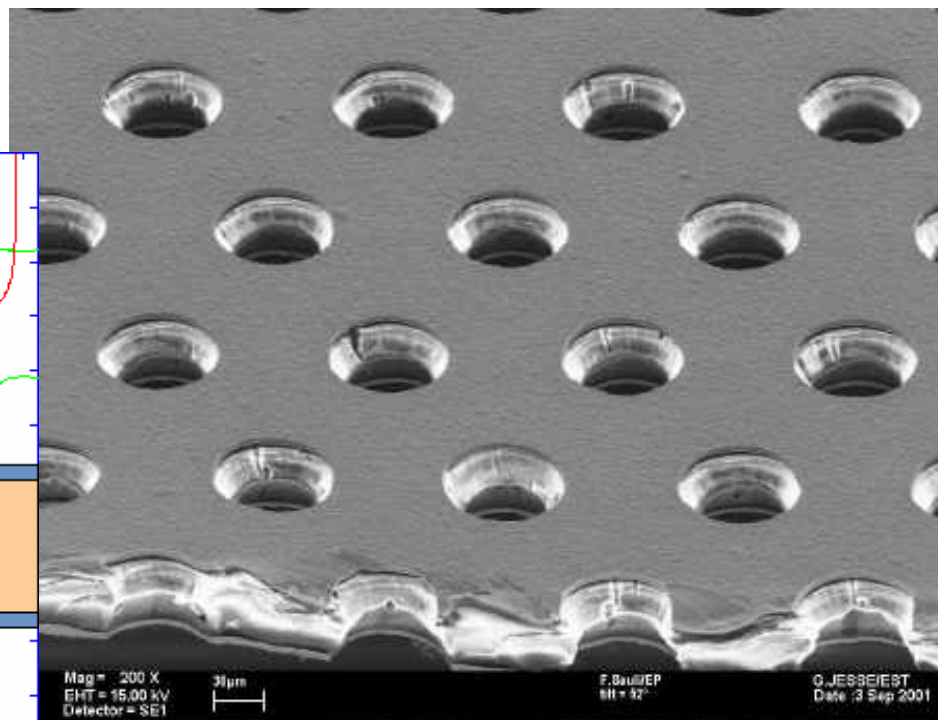
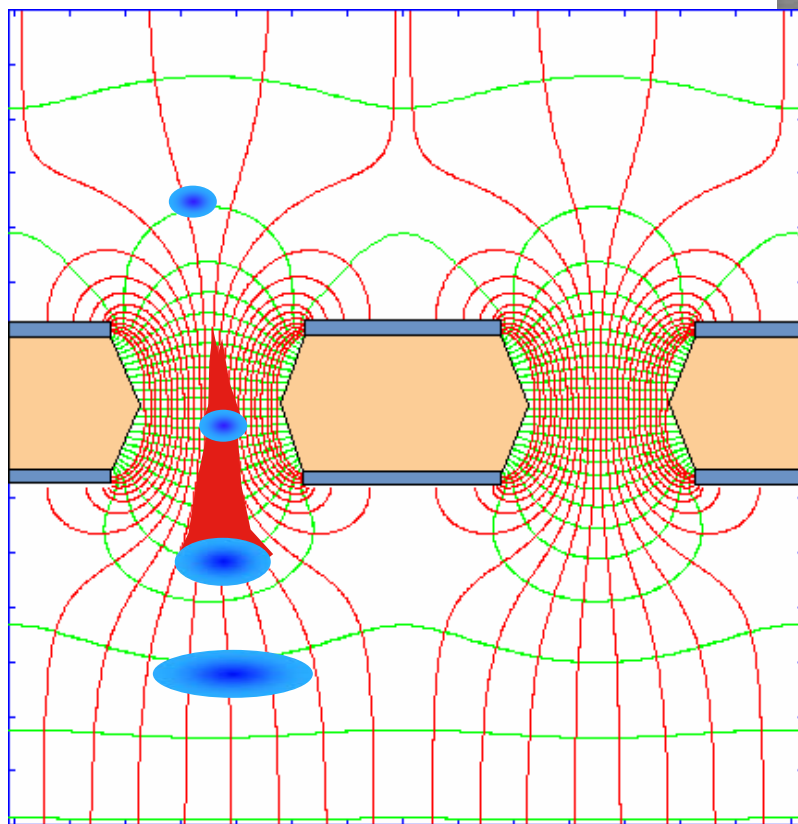
7th International Conference on Position Sensitive Detectors

University of Liverpool, September 16, 2005

GEMs

GAS ELECTRON MULTIPLIER

*THIN, METAL-COATED
POLYMER FOIL WITH A LARGE
DENSITY OF HOLES (100 mm^{-2})*

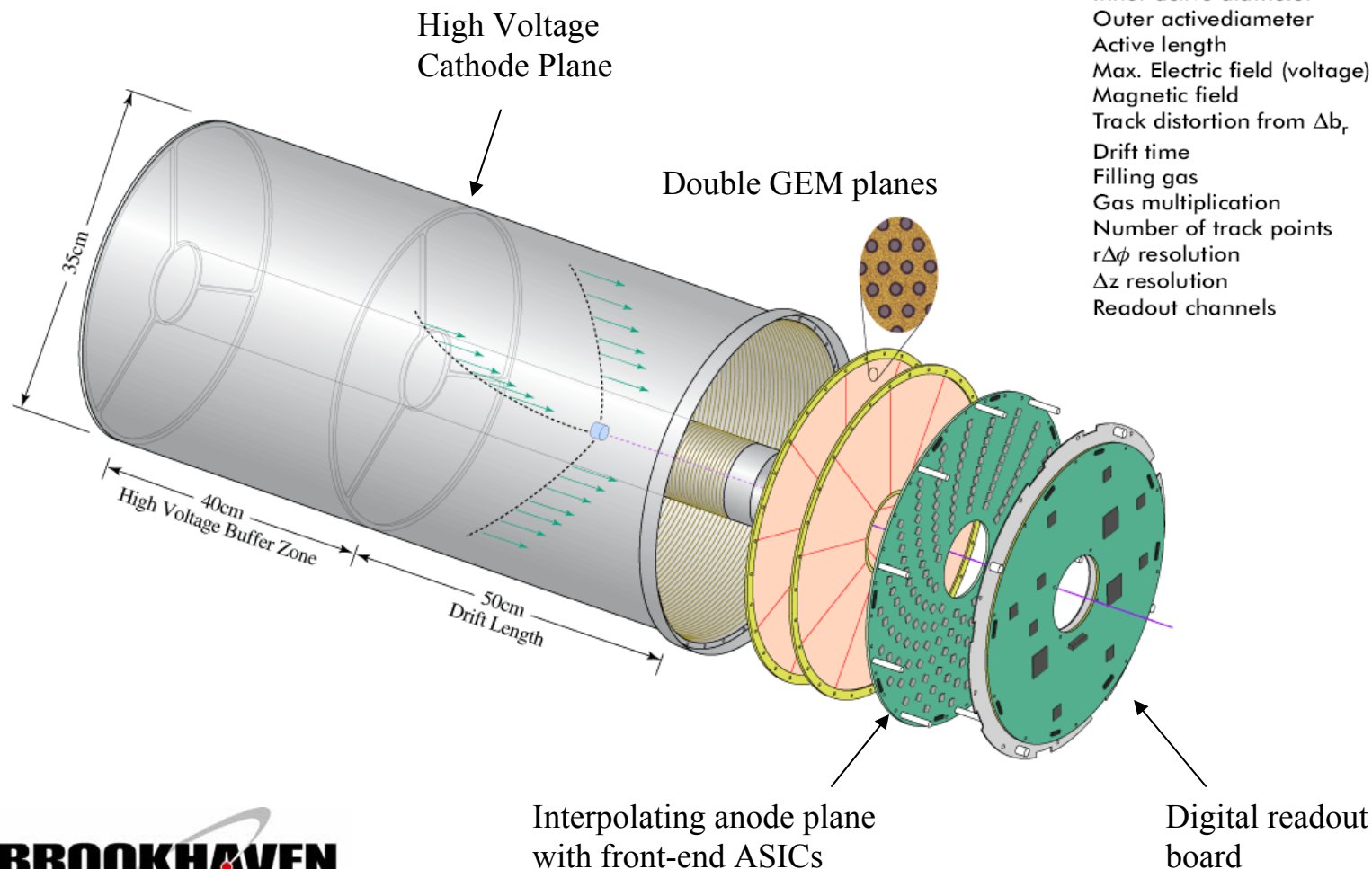


LEGS TPC – Overall view

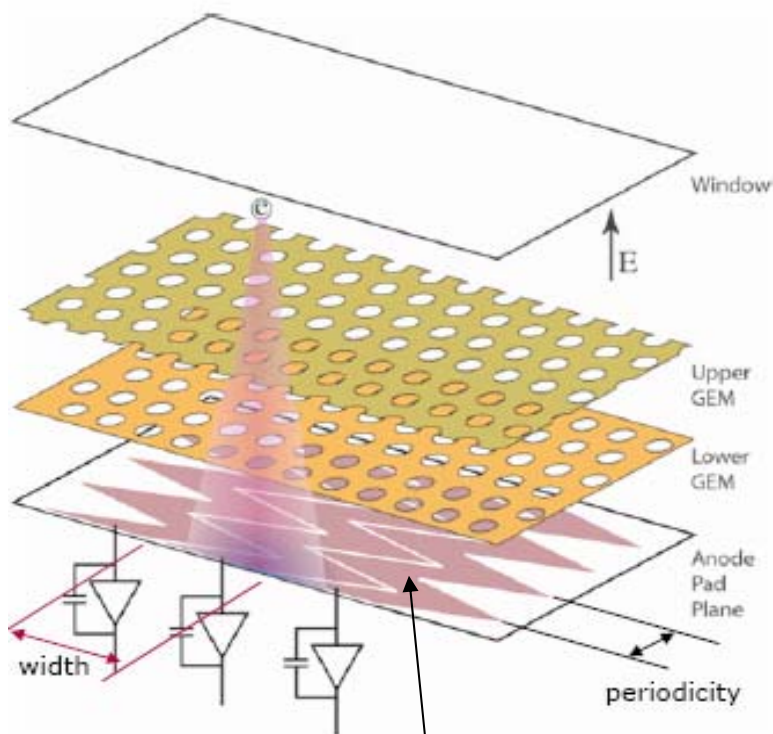
(Laser Electron Gamma-ray Source)

Design Specifications

Available Volume	51.5 x 51.5 x 81.7 cm
Inner active diameter	8.7 cm
Outer activediameter	35.7 cm
Active length	50 cm
Max. Electric field (voltage)	700 V/cm (35kV)
Magnetic field	1.8 T
Track distortion from Δb_r	<1 mm
Drift time	<5 μ s
Filling gas	Ar + CF ₄ + C ₂ H ₆ @ STP
Gas multiplication	low (≤ 1000)
Number of track points	>20 pad rows
$r\Delta\phi$ resolution	<200 μ m
Δz resolution	<20 ns
Readout channels	~8000



LEGS TPC – Interpolating Pad Readout



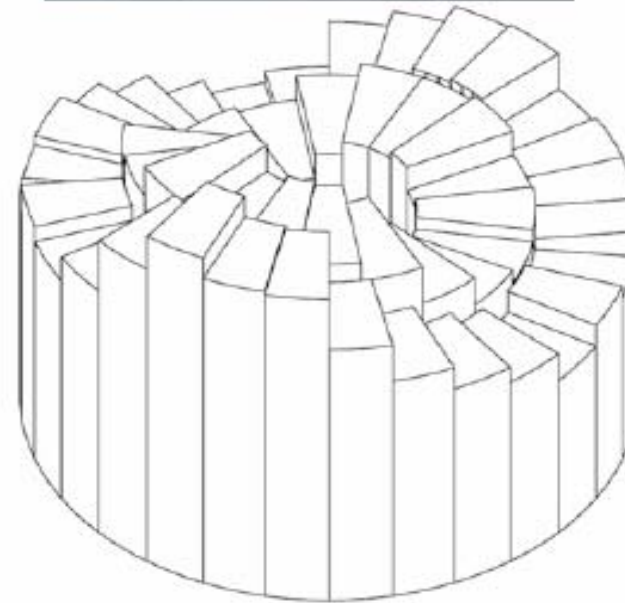
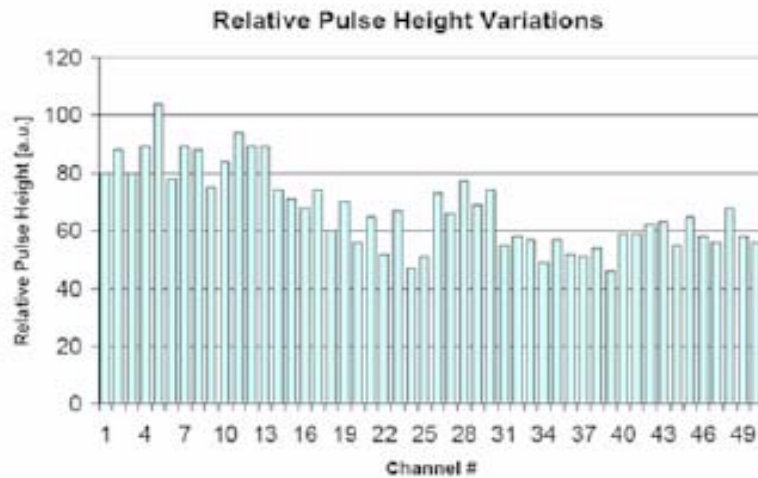
The spread of the electron cloud at the anode pad plane is mostly determined by the diffusion process. It is typically well under 1mm.

A rectangular pad with a width larger than the FWHM of the charge cloud will exhibit large position non-linearity.

A zigzag shaped pad with a zigzag periodicity under 1mm will give good position linearity. The width of the pad can be much larger than the charge cloud.

The interpolating pad plane contains about 8000 of these discrete zig-zag pads

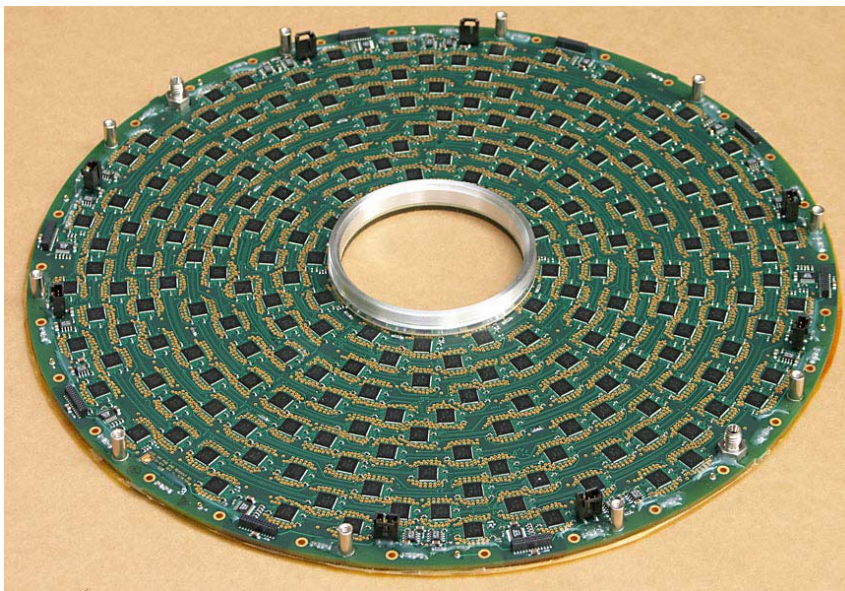
LEGS TPC – Gain Map



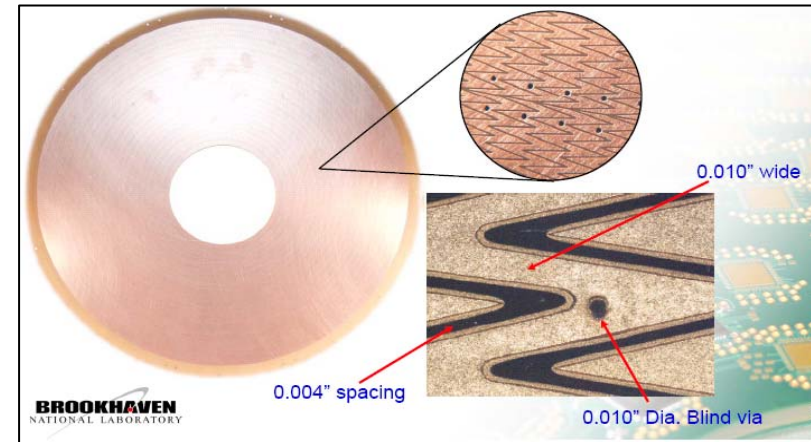
In practice, a more detailed gain map, combined with digital control of ASIC gains, will permit equalization of the combined gas/electronic gain

LEGS TPC – Anode Pad Board

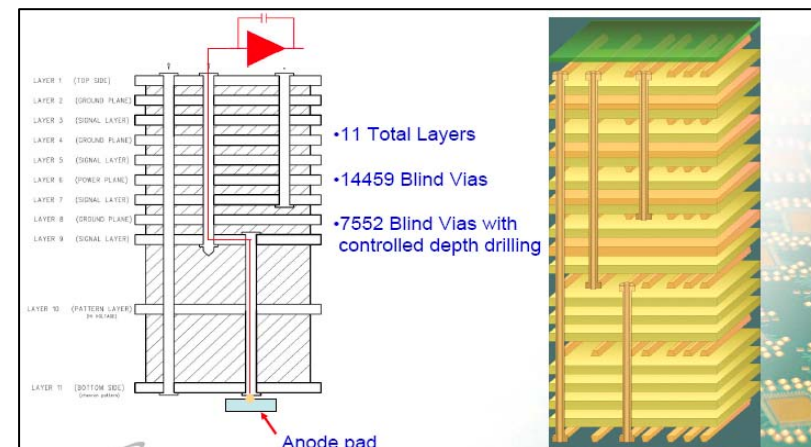
Rear side of anode pad board – each ASIC contains 32 channels, total of about 8000 channels



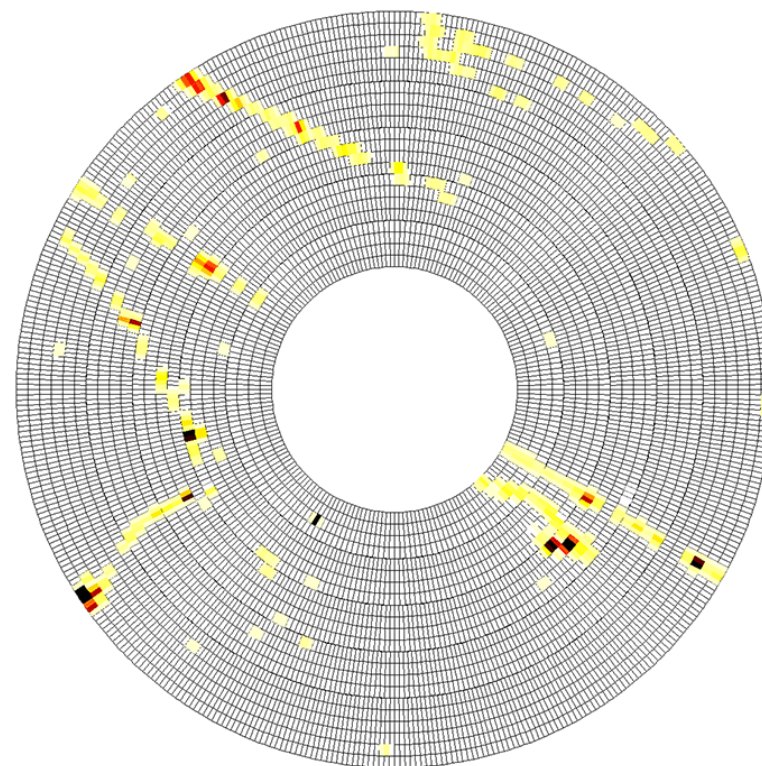
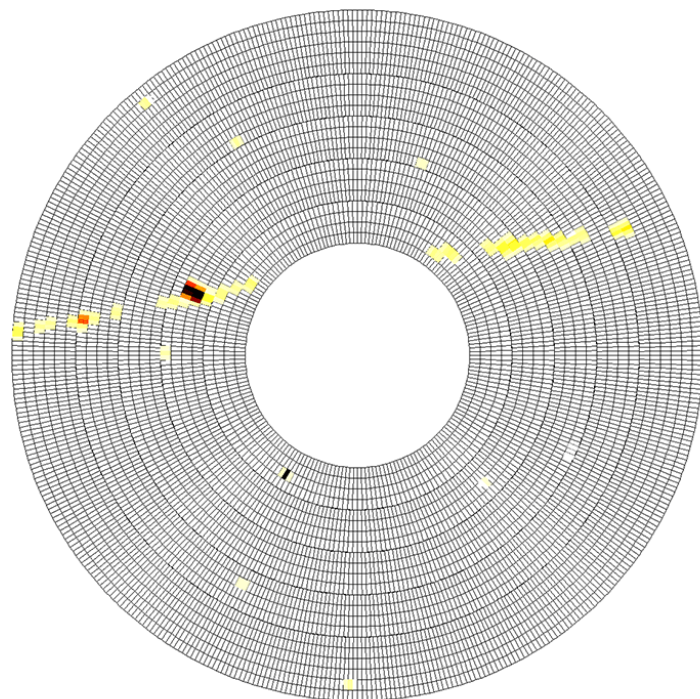
Each pad requires plated hole



Density of pads requires dog-leg in plated through holes



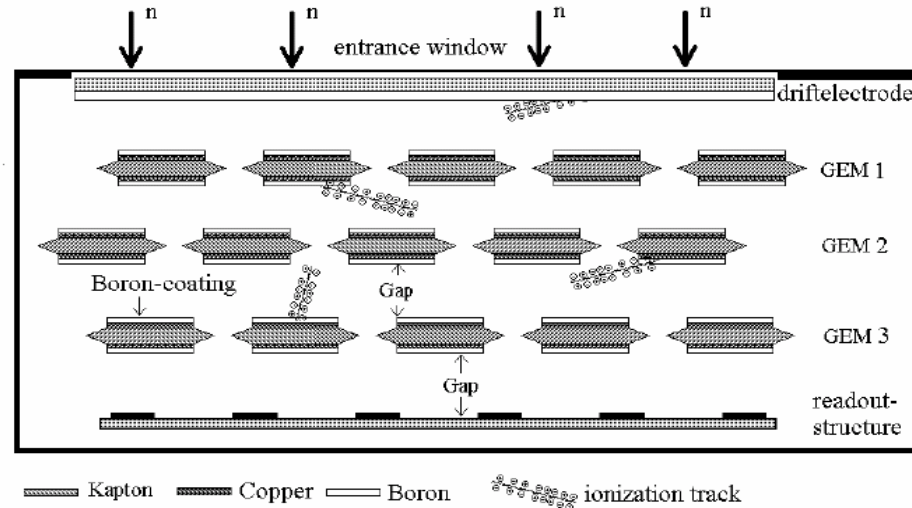
LEGS TPC – Cosmic Ray Tracks



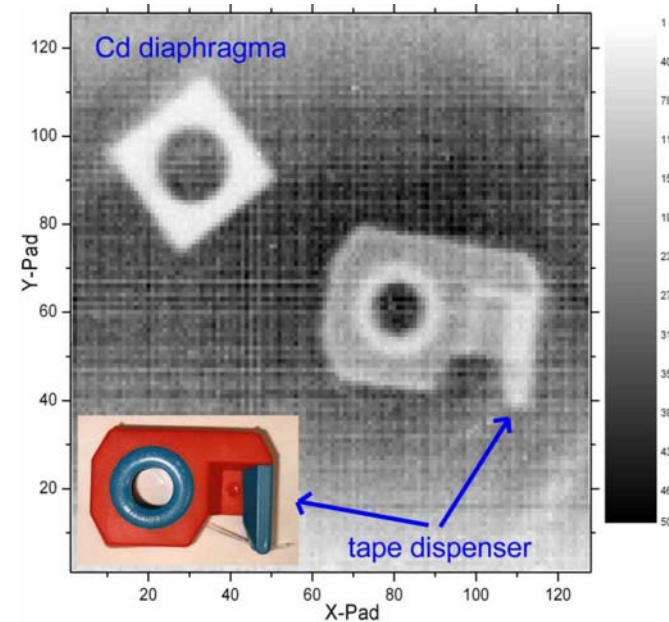
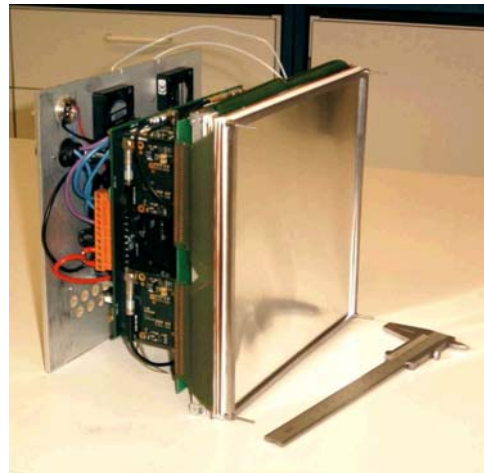
- Threshold per channel: $\sim 1,500$ electrons
- Mean signal level per pad: $\sim 10,000$ electrons

CASCADE Detector for Neutrons

(Klein et al, University of Heidelberg)



200mm by
200 mm
CASCADE
detector



Radiograph of
cadmium
sheet and tape
dispenser
(Cf source,
Heidelberg)

GEM descriptions to follow

Amos Breskin:

THGEMs

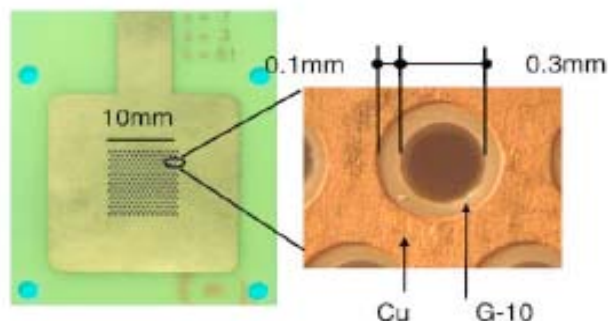


Fig. 1. A photograph of a 0.4 mm thick THGEM with 0.3 mm holes and 0.7 mm pitch. The enlarged part (right) shows the 0.1 mm etched copper edge, preventing discharges at high potentials.

Alison Laird:

Cylindrical GEMs

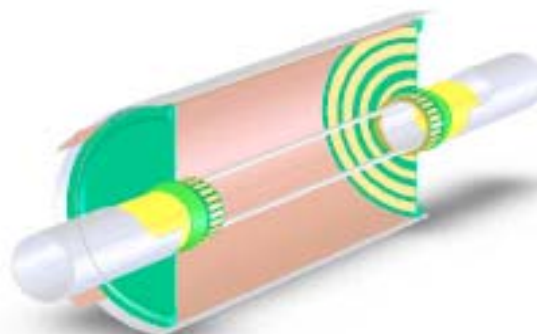
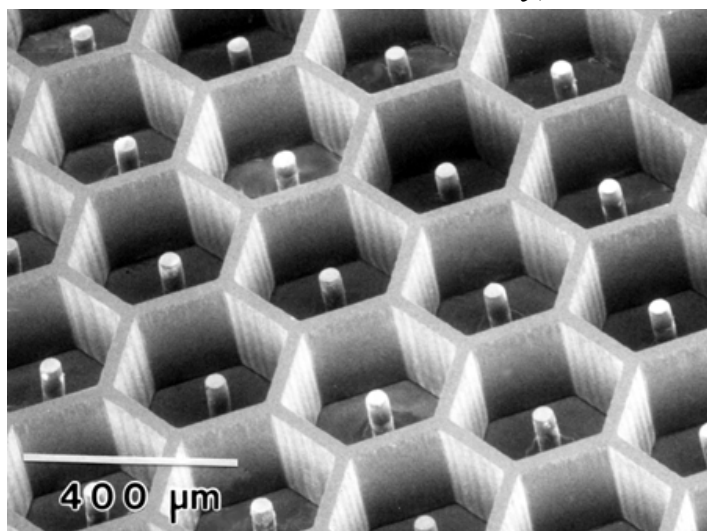


Fig. 2. Three-dimensional cut-away view of proposed TACTIC detector.

Pin Detectors

Rehak et al. IEEE Trans Nucl. Sci 47 (2000) 1426-1429

MIPA _ Micro-Pin Array)



The MIPA electrodes were fabricated from SU-8, an epoxy-based, negative-acting photoresist that displays excellent transparency in the near UV. The relative UV transparency of this resist, when exposed with collimated UV radiation that minimizes lateral scattering, enables the fabrication of microstructures with vertical sidewalls and aspect ratios (sidewall height divided sidewall thickness) of 15:1. A standard chrome-on-quartz mask, typically used for lithography in integrated circuit fabrication, is used to fabricate the MIPA electrode array on an SU-8 layer spun on to a silicon wafer.

Bateman et al, NIM A485 (2003) 596-605

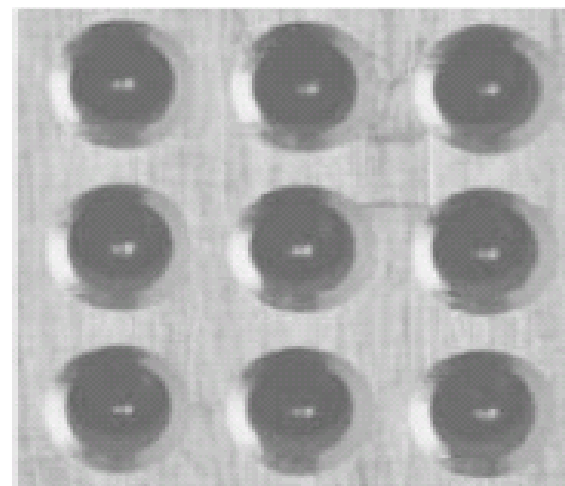


Fig. 2. A photograph of a small portion of the pin array assembly as viewed from the drift space of the detector.

MIPA

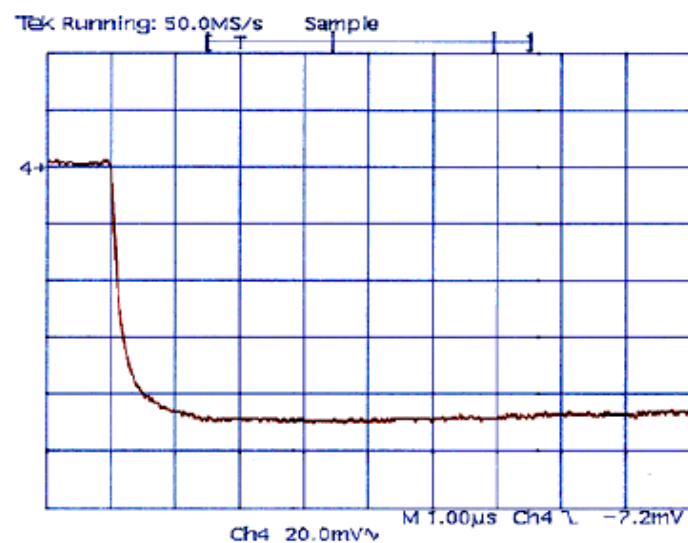


Figure 3: Signal waveform at the output of a charge sensing preamplifier connected to the cathode of the MIPA structure excited by a 5.9 keV X-ray.

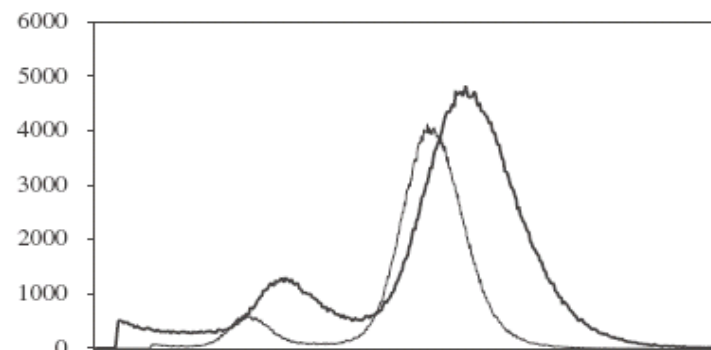


Figure 4: X-ray spectra from MIPA detector. Thin line: one or two cells illuminated by 5.4 keV X-rays. Thick line: entire prototype illuminated by 5.9 keV X-rays.

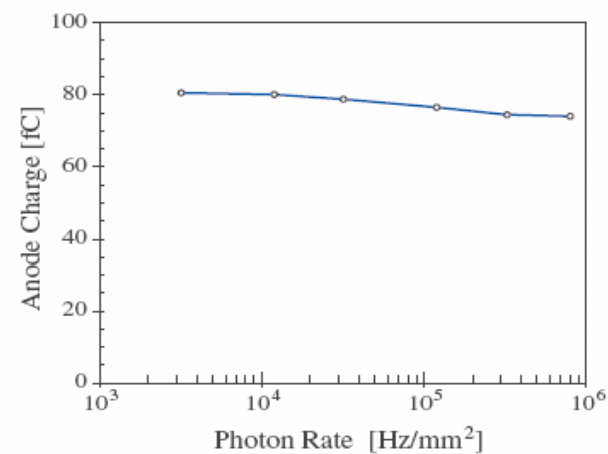


Figure 6: Anode charge as a function of photon rate with a collimated 5.4 keV X-ray beam. The beam size is $25 \mu\text{m} \times 1 \text{mm}$.

MicroCAT (almost a Micromegas)

Ralf menk et al, Trieste and Siegen

μ CAT

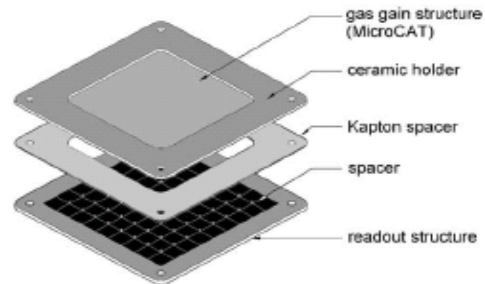


Fig. 1. Inner components of the MicroCAT detector with its interpolating readout structure. The cylindric pin spacers are fixed on the readout nodes.

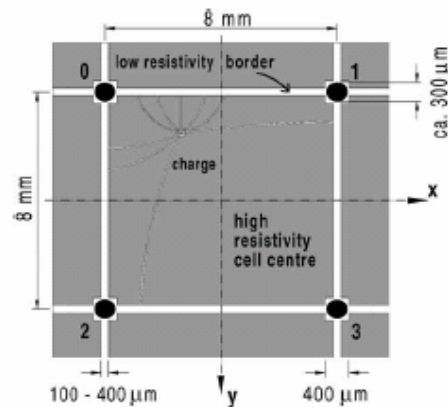
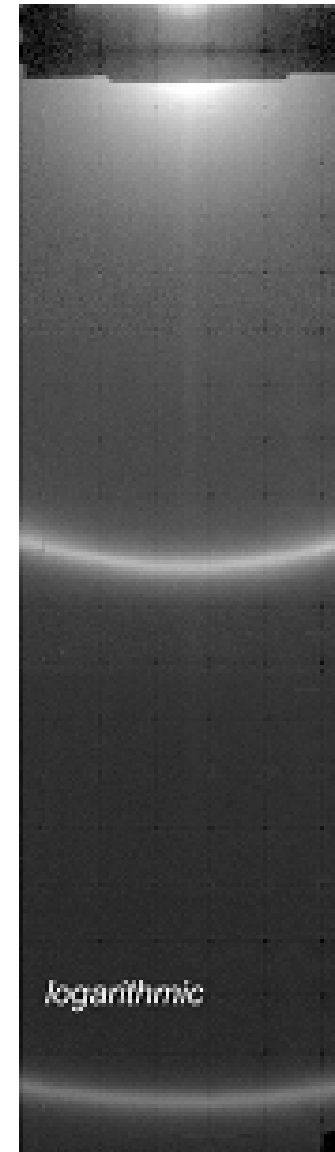
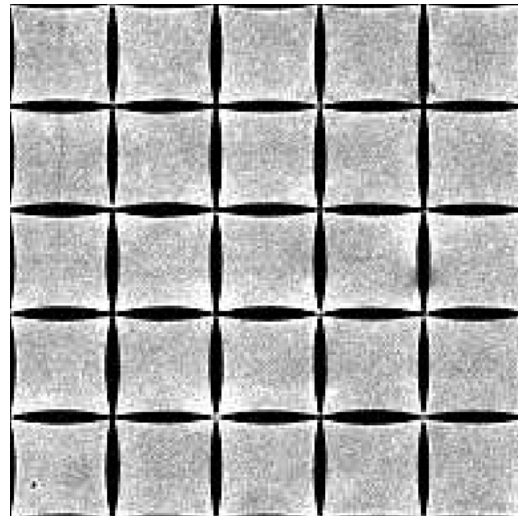


Fig. 2. Schematic illustration of a single cell within the cell collective. The edge length of a cell amounts to $g = 8$ mm. The readout nodes represented by the black circles are placed in the crossing points of the low resistivity strips. The surface resistances of the low resistivity strips R_2 and the high resistivity cell centre R_1 are typically $1-10 \text{ k}\Omega/\square$ and $100 \text{ k}\Omega/\square-1 \text{ M}\Omega/\square$, respectively.



Virtual Pixel



Correction
Matrix

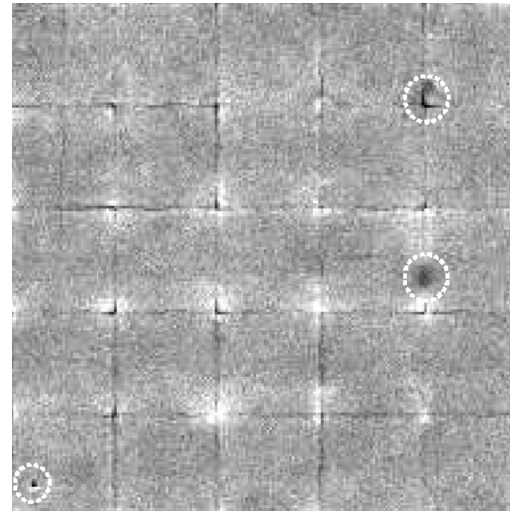
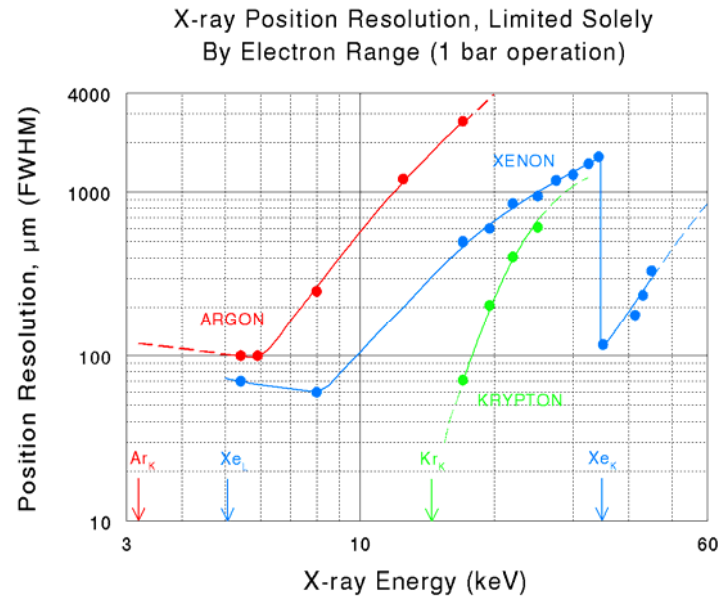


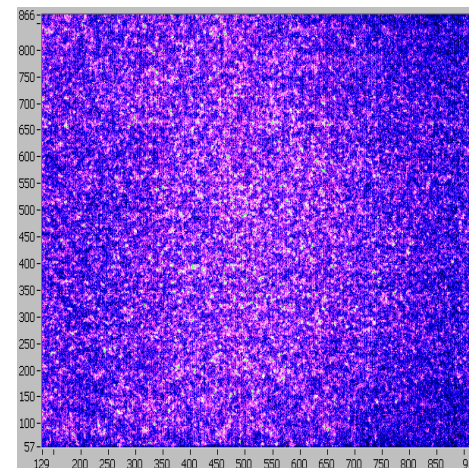
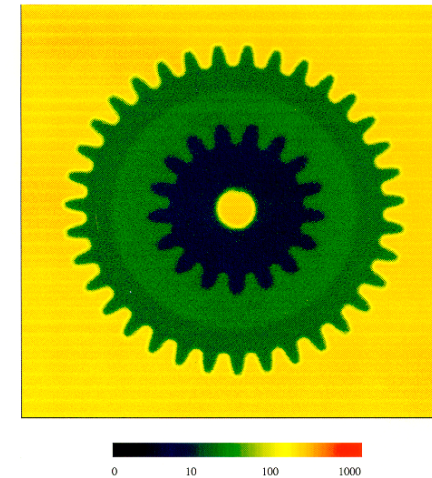
Fig. 18. On the left-hand side the image of the "SAXS" aperture recorded with a PCB-readout structure is shown. On the right-hand side a photo of the aperture taken with a standard digital camera against the sunlight is depicted. The distance between detector and source amounted to about 2.5 m, therefore parallax is very small. The illuminated spots at the bottom correspond to holes in the aperture with diameters of 280, 380, 480, 580 and 680 μm . The aperture is slightly tilted by an angle of about 0.6° , which can be recognised for example by the vertical pixel jump (pixel quantisation) at the bottom of the "2" (dashed-dotted line). The sizes of both depicted images amount to $4.4 \times 4.4 \text{ cm}^2$.

MWPCs with 0.5mm Wire Spacing



At 3 bar, Xe/10%CO₂ will permit resolution of less than 50μm FWHM, which can be achieved provided the signal to noise is as good. This yields a detector for SPECKLE with comparable resolution to CCDs, but no read noise.

Object : 15 mm diameter plastic gear wheel



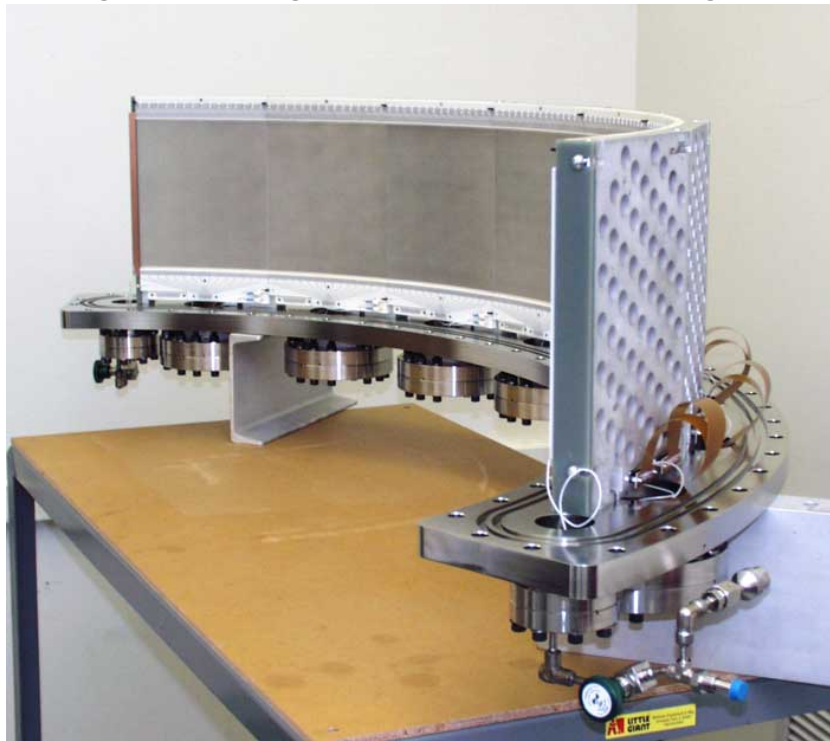
Static speckle patterns
from an aerogel (APS 8-ID)

Experimental Condition

- $E_x = 7.45$ keV
- Aperture slit size: 15 x 15 μm
- Sample-to-detector : 510 cm
- Sample in 10⁻⁴ torr vacuum

120° Two-Dimensional Thermal Neutron Detector for Protein Crystallography

Eight wire-segments mounted on flange



Pressure vessel being lowered



Physics Today, November 2003

Neutron Diffraction Overcomes Flux Limits to Resolve a Large Protein Structure

To demonstrate the effectiveness of neutron diffraction in biology, crystallographers bring neutrons to bear on an important industrial enzyme.

On paper, thermal neutrons seem ideal for probing the structure of crystallized biomolecules. At a few tenths of a nanometer, the de Broglie wavelength of thermal neutrons matches molecular bond lengths. And thermal neutrons interact strongly enough with matter to pick up structural information but weakly enough to pass through crystallites un-

scattered. Scattering strength also varies from isotope to isotope. Conveniently for crystallographers, one of the strongest differences is between hydrogen and deuterium. Substituting deuterium for hydrogen at a specific chemical site reveals the site's spatial location through a simple comparison of diffraction patterns.

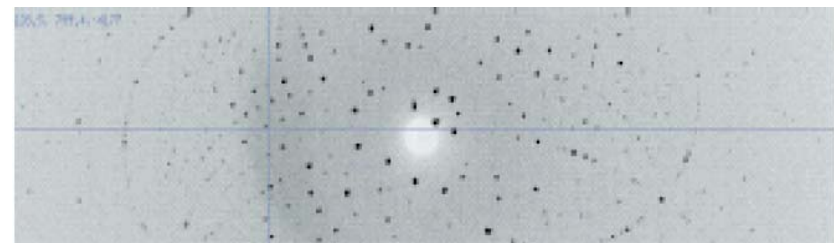
third-generation synchrotrons flood samples with 10^{18} x-ray photons per second per square centimeter; a reactor source, such as the one at the Institut Laue-Langevin in Grenoble, France, emits about 10^{14} neutrons per second per square centimeter.

Because of the relatively low intensity of neutron beams, it takes crystallographers far longer to collect a neutron diffraction pattern than an x-ray diffraction pattern. And more copies of the molecule have to be prepared.

The detector contains eight, independent MWPC segments, providing a continuously sensitive array of about 1/4 million picture elements, and throughput approaching 10^6 n s⁻¹.



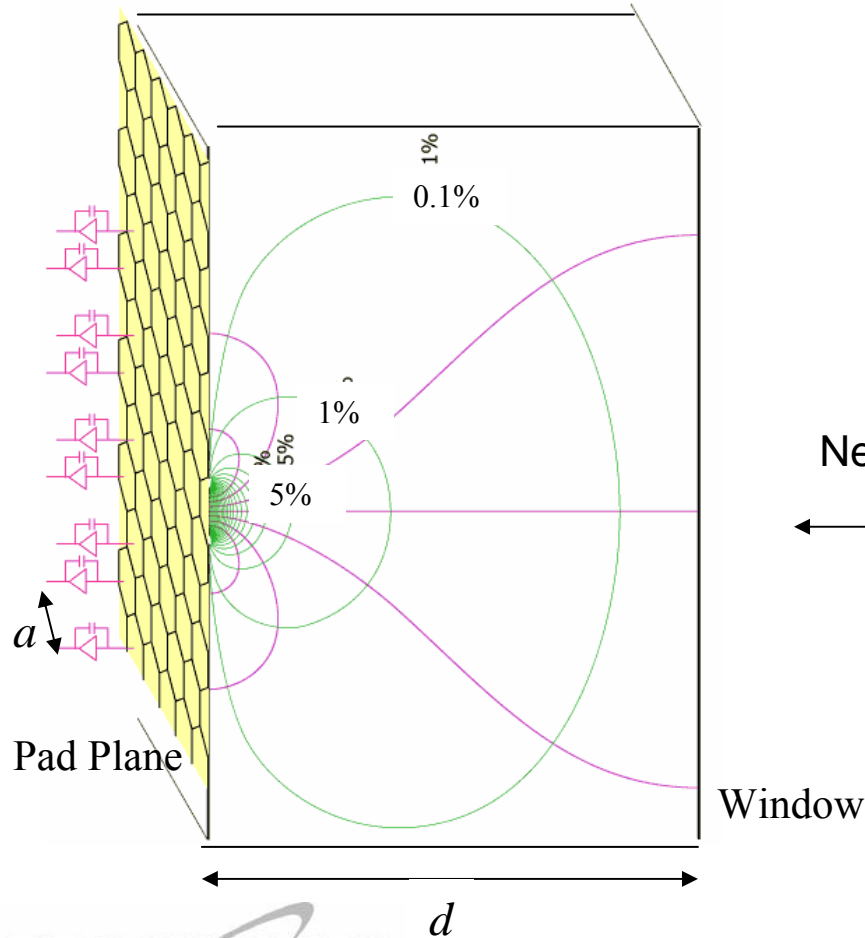
Figure 1. The Protein Crystallography Station at the Los Alamos Neutron Science Center. The sample is held by the rotating stage at the bottom left. Eight detectors are arrayed about 1 meter away from the sample to collect the scattered neutrons. (Courtesy of Gery Bunick.)



D-xylose
isomerase: data-set
from PCS at
LANSCÉ

Two-dimensional, Pad Chamber for Neutrons

Weighting field of a single pad in a parallel plate geometry



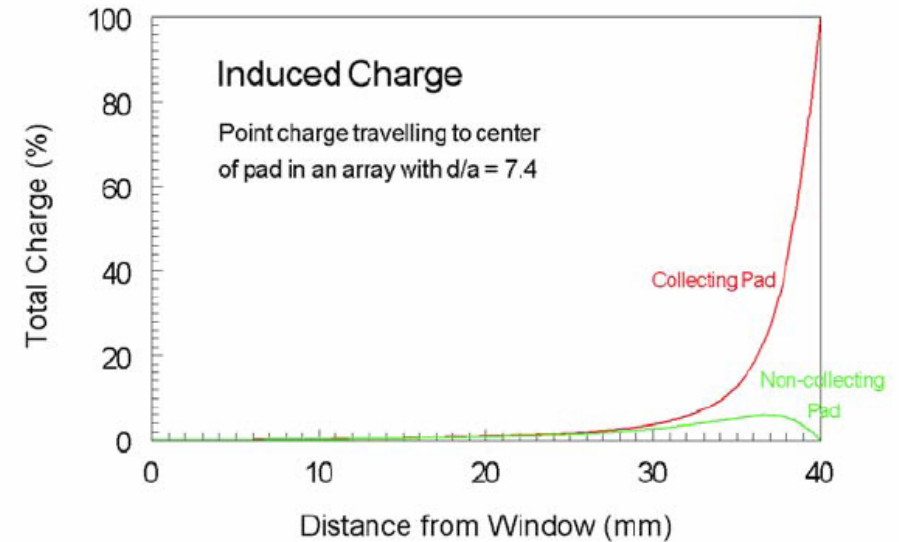
In our first test detector:

Area of each pad = 25mm²

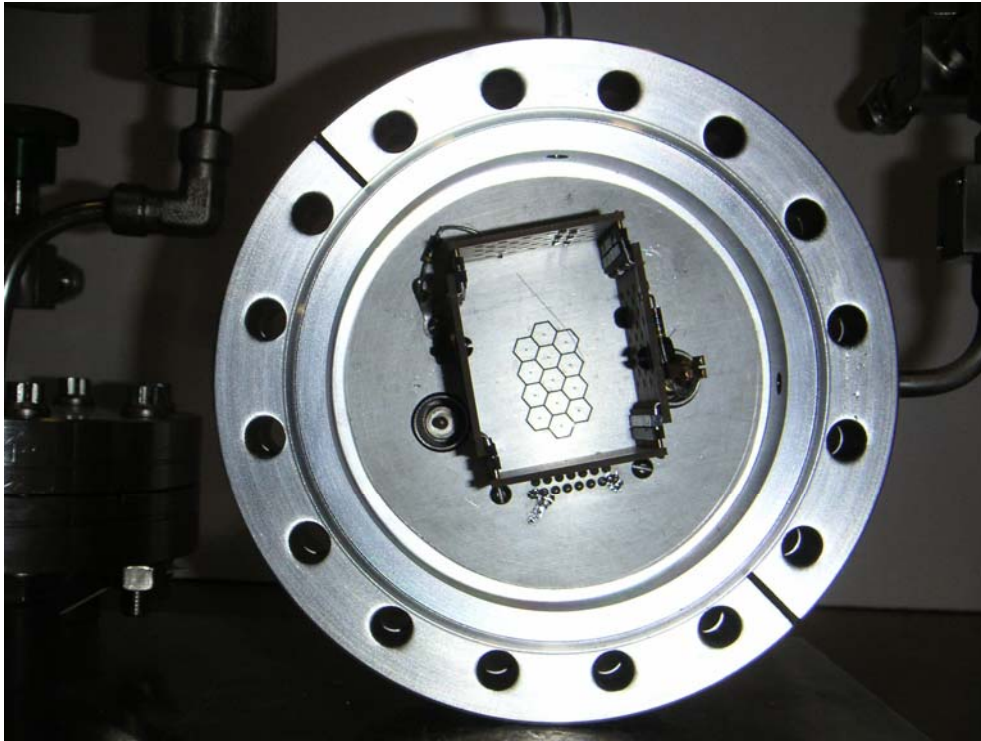
$a = 5.4$ mm

$d = 40$ mm

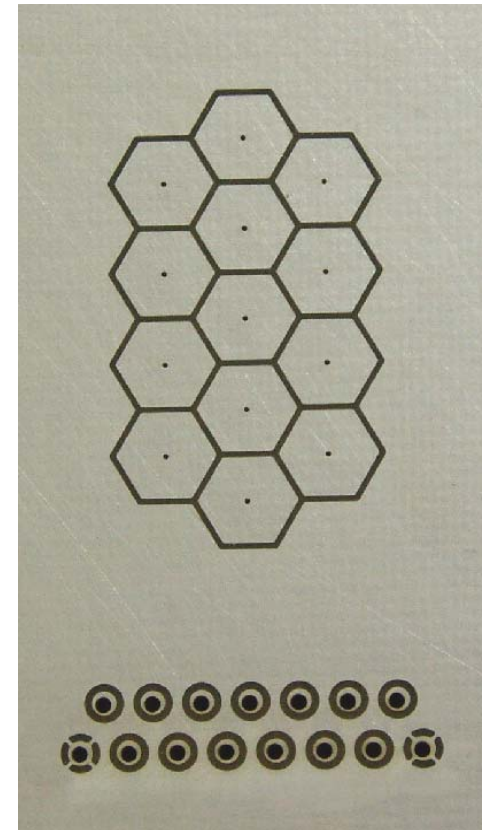
$d/a = 7.4$



Two-dimensional Pad Chamber Prototype Cell

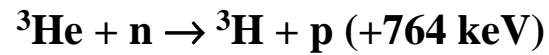


Looking down onto test cell

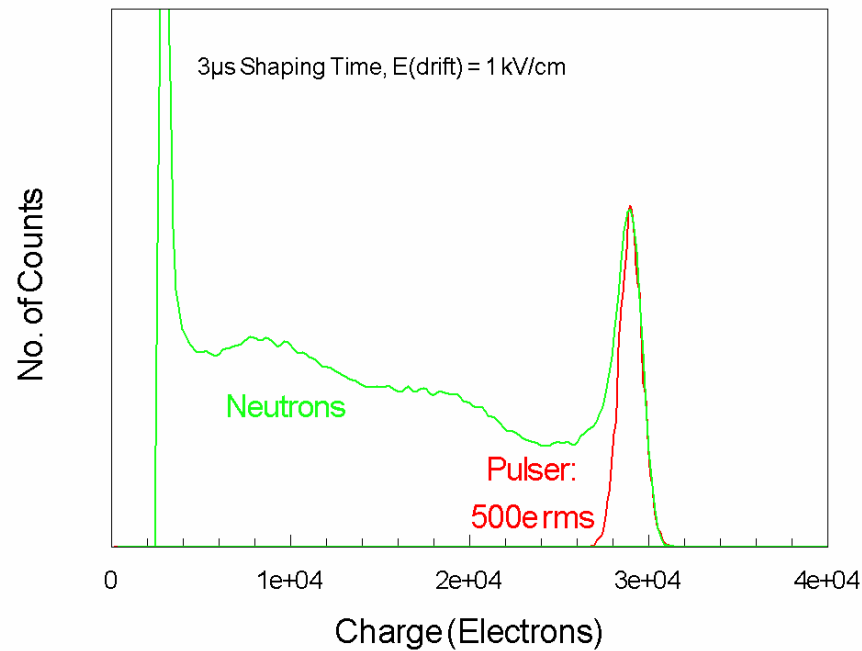


Anode pad board, showing 13 hexagonal pads, 5mm center to center, with printed-through holes (central to each pad) that make connection, on rear side of board, to multi-pin connection at right.

Two-dimensional, Pad Chamber for Neutrons

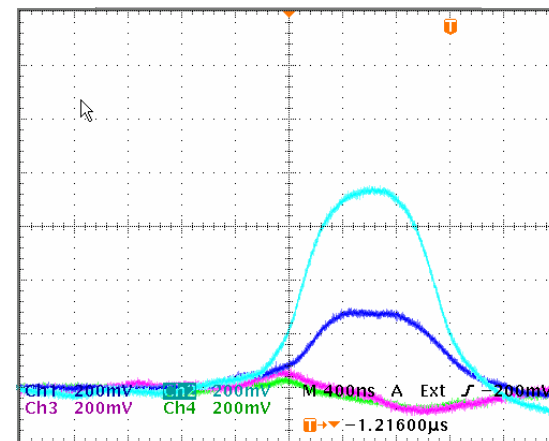
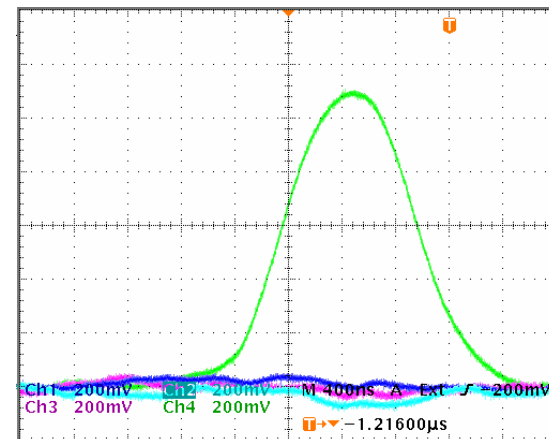


Single pad, 3 bar ${}^3\text{He}$ + 1 bar C_3H_8
and electronic noise contribution



Waveforms from 4 adjacent pads

Uniform neutron irradiation



Two-dimensional, Pad Chamber for Neutrons

- Ultra high count rate capability: 10^5 /s per pixel, $>10^8$ /s per detector
- No gas amplification: No aging effect, Stability and reliability
- Flexible geometry:
- Pixel dimension: $\sim 1 - 5$ mm
- Parallax reduction
- Large area, complex geometry possible
- Reliant on development of low noise ASICs (but less complicated than LEGS TPC)

Detector suitable for SANS

Area: ~ 1 m by 1m

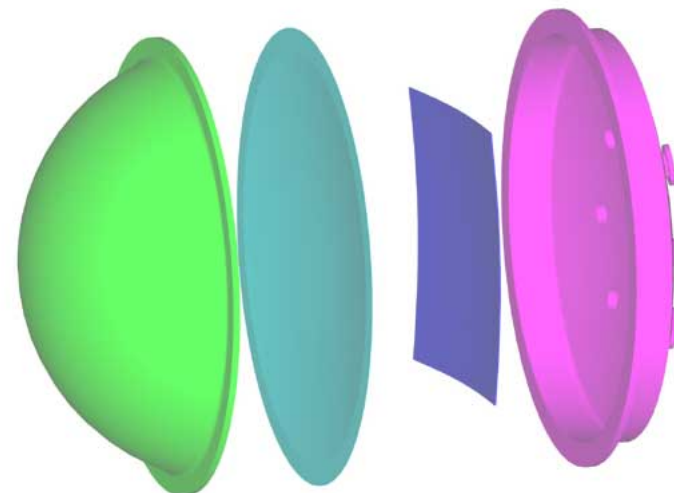
Pixel size: ~ 5 mm by 5mm

Total channel count: $\sim 40,000$

1st level: 64 channels per chip, ~ 625 chips

2nd level digital analysis: ~ 100 feed-throughs

Total power: < 100 W inside detector



Xenon Ionization Detector for Gamma-Ray Spectroscopy

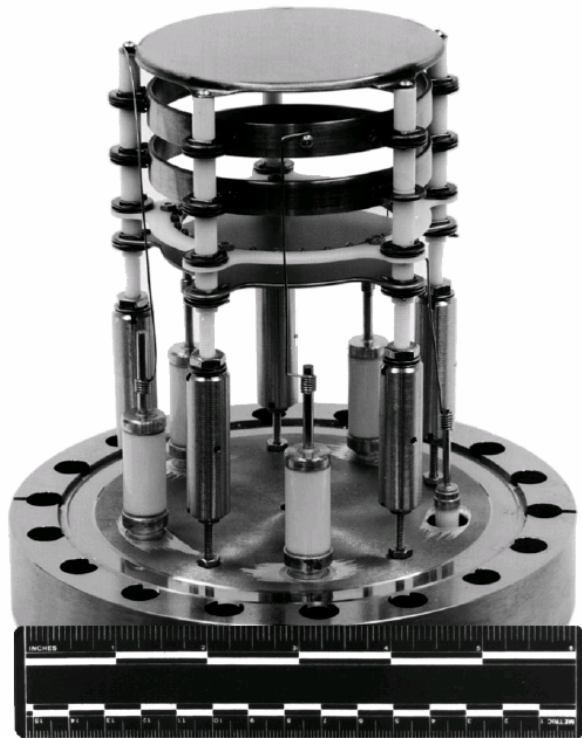
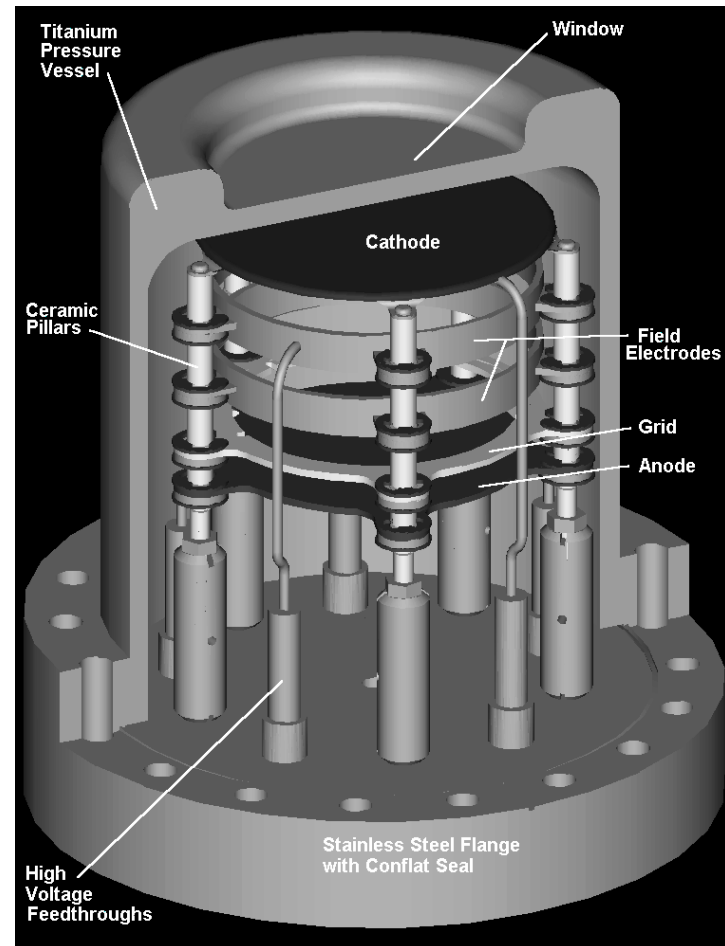
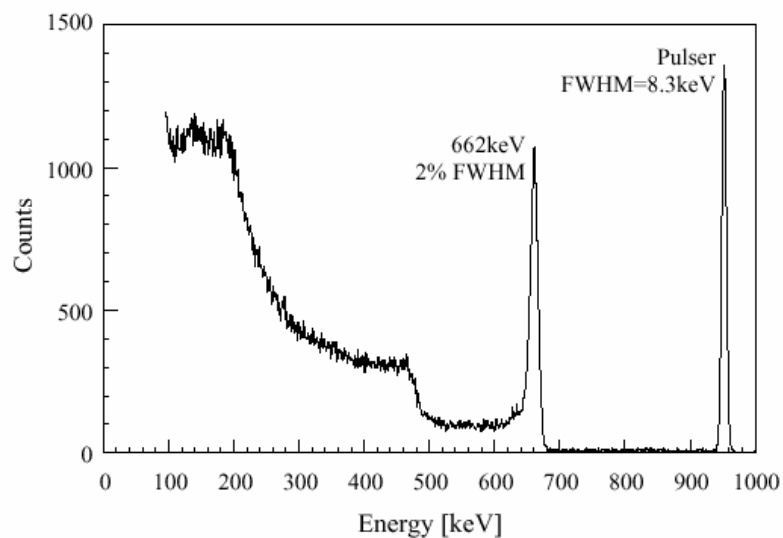


Figure 3. Photograph of internal components of detector vessel, before cover is in place. Cathode, drift electrodes, grid and anode are supported by ceramic pillars, in top half of picture.



Xenon Ionization Detector for Gamma-Ray Spectroscopy

Anode Pulse Height Spectrum: ^{137}Cs



Fano factor limited resolution = 0.55% at 662keV

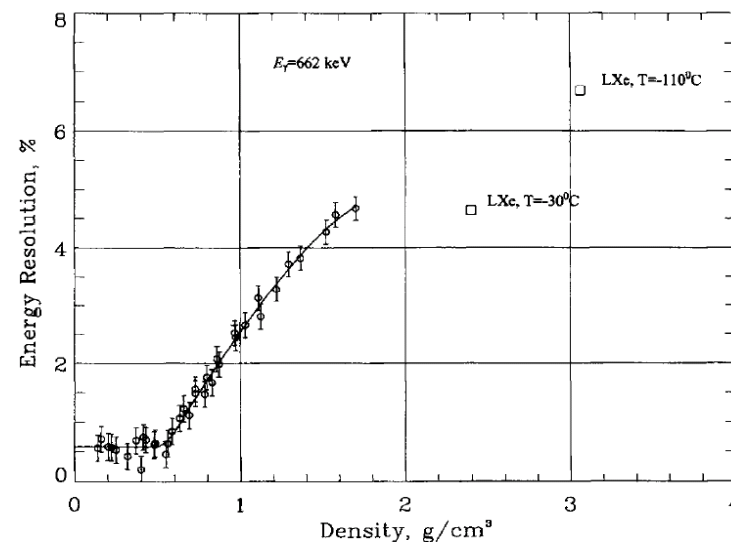


Fig. 5. Density dependencies of the intrinsic energy resolution (%FWHM) measured for 662 keV gamma-rays.

Bolotnikov and Ramsey

The Spectroscopic Properties of High-Pressure Xenon

Nucl. Instrum. & Meth. A396 (1997) 360-370

Summary

- Gas-based detectors provide unique solutions
- Advantages of large area and (more) acceptable cost
- Wire chambers still provide optimum performance
- New micro-structure designs bring additional approaches